Controls on the autochthonous production and respiration of organic matter in cryoconite holes on high Arctic glaciers

Telling, Jon; Anesio, Alexandre Magno; Tranter, Martyn; Stibal, Marek; Hawkings, Jon; Irvine-Fynn, Tristram; Hodson, Andy; Butler, Catriona; Yallop, Marian; Wadham, Jemma

Published in:
Journal of Geophysical Research

DOI:
10.1029/2011JG001828

Publication date:
2012

Citation for published version (APA):
Telling, J., Anesio, A. M., Tranter, M., Stibal, M., Hawkings, J., Irvine-Fynn, T., Hodson, A., Butler, C., Yallop, M., & Wadham, J. (2012). Controls on the autochthonous production and respiration of organic matter in cryoconite holes on high Arctic glaciers. *Journal of Geophysical Research*, *117*(G1), [G01017]. https://doi.org/10.1029/2011JG001828

Controls on the autochthonous production and respiration of organic matter in cryoconite holes on high Arctic glaciers

Jon Telling,[1] Alexandre M. Anesio,[1] Martyn Tranter,[1] Marek Stibal,[1] Jon Hawkings,[1] Tristram Irvine-Fynn,[2] Andy Hodson,[3] Catriona Butler,[1] Marian Yallop,[4] and Jemma Wadham[1]

Received 10 August 2011; revised 14 December 2011; accepted 17 December 2011; published 18 February 2012.

[1] There is current debate about whether the balance of photosynthesis and respiration has any impact on the net accumulation of organic matter on glacier surfaces. This study assesses controls on rates of net ecosystem production (NEP), respiration, and photosynthesis in cryoconite holes during the main melt season (June–August 2009) on three valley glaciers in Svalbard. Cryoconite thickness and organic matter content explained 87% of the total variation in rates of respiration (in units of volume), and organic matter (but not sediment depth) was a significant ($p < 0.05$) control on photosynthesis (by volume). The average rates of respiration and gross photosynthesis within the cryoconite holes were overall closely balanced, ranging from net autotrophic to heterotrophic. Sediment depth explained over half the variation of NEP, with net autotrophic rates typical only in sediment <3 mm thick. The measured rates of NEP were not sufficient to account for the organic matter which has likely accumulated in the cryoconite on timescales of less than decades, suggesting three alternatives for the source of the organic matter. First, the glacier surface may have received windblown allochthonous organic material from surrounding environments. Second, cryoconite may consist of in-washed autochthonous material from the glacier surface which has comparable organic carbon content. Third, much of the organic matter may have accumulated in the hole during a nascent period, when rates of NEP were much higher. The cycling of autochthonous labile carbon produced by phototrophs may sustain a significant proportion of the total in situ microbial activity within cryoconite holes.

Citation: Telling, J., A. M. Anesio, M. Tranter, M. Stibal, J. Hawkings, T. Irvine-Fynn, A. Hodson, C. Butler, M. Yallop, and J. Wadham (2012), Controls on the autochthonous production and respiration of organic matter in cryoconite holes on high Arctic glaciers, *J. Geophys. Res.*, *117*, G01017, doi:10.1029/2011JG001828.

1. Introduction

[2] The origin of organic matter on glacier surfaces is a matter of current debate. One explanation is that a significant fraction of the organic matter is autochthonous; that is, produced in situ by photosynthesis on glaciers [*Anesio et al.*, 2009]. The autochthonous organic matter may then be an important source of organic carbon and nutrients for in situ and downstream ecosystems [*Anesio et al.*, 2009; *Hood et al.*, 2009]. The alternative possibility is that the organic matter is derived dominantly from allochthonous (i.e., external) sources [*Stibal et al.*, 2008a], and the role of microbial activity is relegated to the transformation of preexisting allochthonously derived organic matter [*Hodson et al.*, 2010a]. In both cases, organic matter produced by photosynthesis may cause a decrease in the albedo (and hence melting) of glacier surfaces either directly by the production of dark microbial pigments (e.g., UV-protective compounds such as scytonemin and mycosporine-like amino acids) [*Quesada et al.*, 1999] or indirectly through the trapping of dark debris via the production of exopolysaccharides [*Takeuchi et al.*, 2001; *Hodson et al.*, 2010a].

[3] Microbial activity on the surfaces of glaciers and ice sheets is concentrated in surface sediment, known as cryoconite [*Säwström et al.*, 2002; *Anesio et al.*, 2009]. Cryoconite is primarily composed of inorganic debris, derived either from aeolian dust deposition or locally derived debris from moraines or basal ice [*Takeuchi et al.*, 2001; *Bøggild et al.*, 2010]. The remaining organic fraction is typically <5% by weight [*Takeuchi et al.*, 2005; *Hodson et al.*, 2010a], although values as high as 13–20% have been reported on the Greenland Ice Sheet [*Gerdel and Drouet*, 1960]. A variety of studies have demonstrated that cryoconite contains a wide

[1]Bristol Glaciology Centre, School of Geographical Sciences, University of Bristol, Bristol, UK.
[2]Centre for Glaciology, Institute of Geography and Earth Science, Aberystwyth University, Aberystwyth, UK.
[3]Department of Geography, University of Sheffield, Sheffield, UK.
[4]School of Biological Sciences, University of Bristol, Bristol, UK.

0148-0227/12/2011JG001828

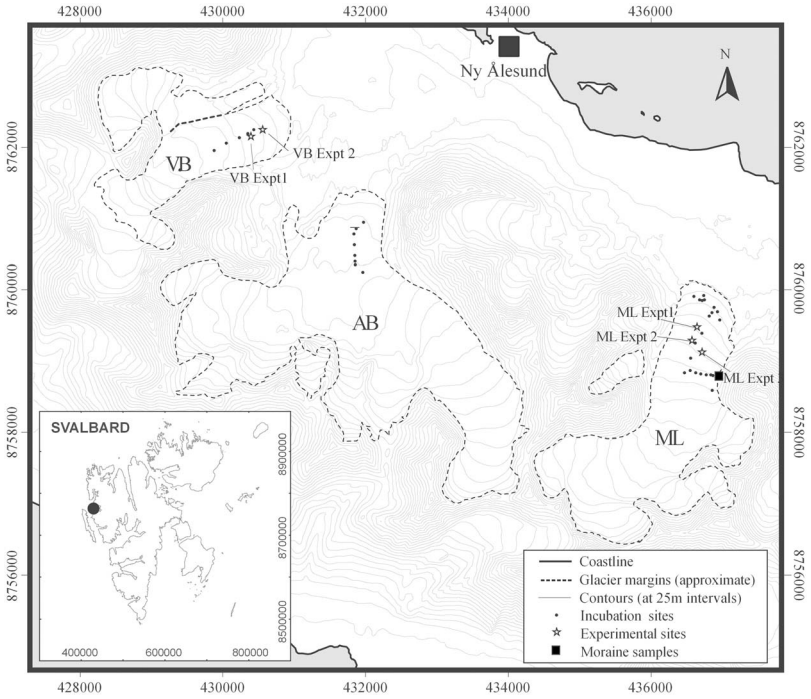

Figure 1. Map showing location of cryoconite holes used for in situ incubations, moraine samples, and cryoconite thickness experimental sites on Austre Brøggerbreen (AB), Midtre Lovénbreen (ML), and Vestre Brøggerbreen (VB). Latitude, 79°N; longitude, 12°E. The map is projected in universal transverse Mercator (UTM) World Geodetic System (WGS 84) with contours displayed at 100 m intervals.

diversity of prokaryotic and eukaryotic microorganisms, including both heterotrophs and phototrophs. The latter includes both cyanobacteria and green algae [*Christner et al.*, 2003; *Stibal et al.*, 2006; *Edwards et al.*, 2011].

[4] In this study we measured in situ rates of net ecosystem production (NEP), respiration and gross photosynthesis in cryoconite holes on three valley glaciers in Svalbard during the main summer melt season in 2009. Potential environmental controls on microbial productivity rates are identified by multivariate statistical analyses of site, sediment thickness, organic carbon and chlorophyll *a* data. Further batch experiments were carried out to directly quantify the effects of cryoconite thickness on rates of microbial activity. The significance of photosynthesis for producing organic matter within cryoconite holes and supporting in situ microbial activity is assessed.

2. Methods

2.1. Study Sites

[5] Incubation experiments were conducted with cryoconite from three neighboring, north-facing valley glaciers, Midtre Lovénbreen (ML), Vestre Brøggerbreen (VB) and Austre Brøggerbreen (AB), situated in the NW of the Svalbard archipelago, close to the scientific base at Ny-Ålesund at 79°N 12°E (Figure 1). All three glaciers have exhibited sustained negative mass balance since the 1930s resulting in retreat and ice thinning with large proportions of the ice area below the long-term mean snowline elevation [*Hagen et al.*, 2003; *Nuth et al.*, 2007]. Incubations took place between 13 July to 25 August 2009. All incubations were carried out on the surface of the glaciers, either within cryoconite holes (to estimate in situ rates of net ecosystem production (NEP), gross photosynthesis and respiration) or on the surface of the glaciers (for experimental manipulations on cryoconite thickness). Therefore, all incubations were conducted under in situ light and temperature conditions. All of the studied cryoconite holes were open to the atmosphere (i.e., the holes were not covered by slush or ice). The majority of cryoconite holes had a measurable flow through of water (i.e., stream cryoconite holes). Three samples of moraine debris were also sampled from a lateral moraine on the eastern periphery of ML on 25 August 2009 (Figure 1).

2.2. In Situ Rates of Net Ecological Production, Gross Photosynthesis, and Respiration

[6] Rates of NEP, gross photosynthesis and respiration were measured at a total of 40 cryoconite holes on the three different glaciers (AB, ML, VB; see Figure 1). All manipulations and analyses were carried out on the surface of the glaciers, and closed bottle incubations carried out within the respective cryoconite holes. Cryoconite was removed from each hole using a plastic scoop, and immediately added to two glass bottles with tapered glass stoppers (65 mL BOD bottles, Wheaton). Care was taken to replicate the average in situ cryoconite thickness in the incubation bottles. All bottles were completely filled with in situ supraglacial water using a 60 mL plastic syringe, leaving no headspace in the bottles. One of the two bottles at each site was covered with aluminum foil (dark bottle). The remaining bottle was left uncovered (light bottle). In addition, at 26 sites two bottles (one light, one dark) were filled completely with supraglacial

water without sediment, to act as water only controls. The bottles were then completely submerged in water within their corresponding cryoconite holes and incubated for 24 (±3) h.

[7] Start and end concentrations of dissolved inorganic carbon (DIC) and oxygen were measured in incubation bottles using the method of *Telling et al.* [2010]. Measurements were made on the surface of the glaciers immediately after removing each bottle from its respective cryoconite hole. Rates of NEP and respiration in incubation bottles were calculated from the change in DIC (ΔCO_2 method) and oxygen (ΔO_2 method) in light and dark bottles, respectively. Rates of gross photosynthesis were calculated by subtracting the change in DIC (or oxygen) of dark bottles from the change in DIC (or oxygen) of light bottles, after correcting for any differences in dry weights of cryoconite in the dark and light bottles. The detection limits (defined as two × standard error of the mean of six supraglacial water samples) were 18 μg C L^{-1} d^{-1} (ΔCO_2 method) and 96 μg C L^{-1} d^{-1} (ΔO_2 method) for rates of NEP and respiration. The detection limit for gross photosynthesis was 26 μg C L^{-1} d^{-1} (ΔCO_2 method) and 136 μg C L^{-1} d^{-1} (ΔO_2 method) combining errors for the light and dark bottles using the least squares method. The precision of the methods was assessed in a previous study on eleven cryoconite holes on the same three glaciers in the same field season [*Telling et al.*, 2010]. The mean coefficient of variation (CV) was 16.5% ± 7.8% (1σ), 32.0 ± 18.8%, and 32.8 ± 22.0% for rates of respiration, photosynthesis, and NEP, respectively, using the ΔCO_2 method. The mean CV was 29.7 ± 21.7%, 19.2 ± 7.9, and 48.6 ± 54.7% for rates of respiration, photosynthesis, and NEP, respectively, using the ΔO_2 method.

2.3. Cryoconite and Moraine Sampling and Analysis

[8] At each incubation site (Figure 1), the physical dimensions of the cryoconite holes (length, width, depth of water column, thickness of cryoconite debris) were measured using a graduated rule. Cryoconite hole areas were estimated by assuming all holes were circular, using the mean of width and length to estimate the hole circumference. Cryoconite at each site (and moraine debris from the lateral moraine on ML; see Figure 1) was placed into sterile polypropylene centrifuge tubes using plastic scoops. Samples were transported chilled back to the field laboratory at Ny-Ålesund within 8 h of collection, and subsequently frozen (−20°C) and transported back to Bristol for later analysis.

[9] For total organic carbon analysis (TOC) cryoconite and moraine debris was dried in an oven at 70°C for 2 days. Duplicate samples were then analyzed for total carbon (TC) on a Eurovector EA3000 Elemental Analyzer and inorganic carbon (IC) on a Coulomat 720 analyzer. total organic carbon (TOC) was defined as the difference between TC and IC. Duplicate TOC values for cryoconite samples were all within 10% of each other, duplicate moraine samples were between 10% and 19% of each other. The detection limit was 100 μg C g^{-1} dry sediment.

[10] Chlorophyll *a* was analyzed following the method of *Thompson et al.* [1999]. Blanks (ethanol only) were run every 10 samples. Absorption values were standardized against purified chlorophyll *a* from cyanobacteria (Sigma). The detection limit was 100 μg L^{-1} chlorophyll *a*. After normalizing to dry cryoconite weight (μg C g^{-1} d^{-1}), the precision (CV) of duplicate chlorophyll *a* analyses was 9.3 ± 6.7% (1σ).

2.4. Multivariate Statistical Analysis of Field Data

[11] Constrained ordination analysis allows direct assessment of the relationship between known environmental variables and variation in the multivariate data, and was used here to assess the effect of locality, cryoconite sediment thickness and the concentrations of organic carbon and chlorophyll *a* in the sediment on the measured microbial activity (NEP, respiration, photosynthesis).

[12] The data were transformed prior to analysis as follows: glaciers (AB, VB, ML) were used as dummy variables in the analysis; the TOC and chlorophyll *a* data were ln(x + 1) transformed; the sediment thickness data were left untransformed. Since the NEP data contained both negative and positive numbers, they were first multiplied by −1 and then a constant was added resulting in all numbers being positive. These data were then ln transformed, as were the photosynthesis and respiration data. All data were standardized and centered. Samples with any missing data were removed from analysis.

[13] Detrended canonical correspondence analysis (DCCA) was used first to determine the length of the gradient along the first ordination axis, in order to select the appropriate method for constrained ordination of the data [*ter Braak and Šmilauer*, 2002]. Redundancy analysis (RDA) was then used to evaluate the significance of the environmental variables (glacier, sediment thickness, TOC, chlorophyll *a*) as controls for biological processes, using the approach of *Kaštovská et al.* [2005]. RDA is a constrained ordination technique, based on principal component analysis (PCA), in which ordination axes are constrained to be linear combinations of environmental variables. The significance of the relationship is tested with the Monte Carlo permutation test [*ter Braak and Šmilauer*, 2002]. The following RDA setup was used: focus on sample distances, 499 unrestricted Monte Carlo permutations, and manual forward selection. In forward selection, the construction of the regression model starts with the environmental variable that explains the most variation in the dependent variables. What remains of the variation to explain after fitting the first variable is then used to choose the second environmental variable. The process of selection goes on until no more variables significantly explain the residual variation. This allows to select the most significant variables and to avoid the problem of multicollinearity [*Legendre and Legendre*, 1998; *Ramette and Tiedje*, 2007].

[14] All the analyses were performed in the multivariate data analysis software CANOCO 4.5. The program CANODRAW 4.0 [*ter Braak and Šmilauer*, 2002] was used for graphical presentation of ordination results. The results of RDA were summarized using a biplot diagram, in which the relative length and position of arrows show the extent and direction of response of the selected dependent variables to the environmental factors.

2.5. Cryoconite Thickness Experiments

[15] Five experiments (ML Expt 1–3, VB Expt 1–2; see Figure 1) were set up to specifically investigate the dependence of rates of NEP and gross photosynthesis on cryoconite thickness. Bottle incubations were set up exactly as described

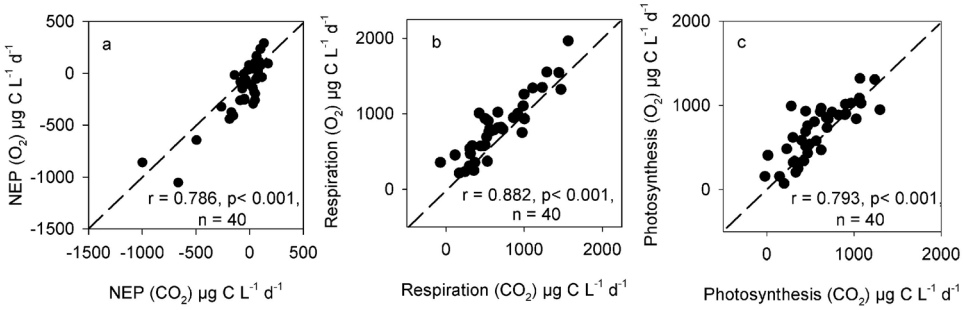

Figure 2. Scatterplots showing correlations between ΔCO_2 and ΔO_2 measurements in cryoconite holes for (a) net ecological production (NEP), (b) respiration, and (c) photosynthesis. Here r values are determined by Spearman's correlation, and p values are determined from two-tailed t tests.

above for the in situ measurements, with the exceptions that (1) a range of different cryoconite thicknesses were used (0.5/1.0 to 8.0 mm, with the former values representing one grain thick cryoconite layers) and (2) the bottles were incubated on the glacier surface rather than submerged at the bottom of cryoconite holes. As before, all manipulations and analyses were performed on the surface of the glaciers. In each experiment, a light and dark bottle was set up for each cryoconite thickness, along with water only controls.

3. Results

3.1. Microbial Activity

[16] There were significant positive correlations between the ΔO_2 and ΔCO_2 methods for NEP ($r = 0.786$; $p < 0.001$; $n = 40$; Spearman's correlation; two-tailed t test), respiration ($r = 0.882$; $n = 40$; $p < 0.001$; Spearman's correlation; two-tailed t test) and photosynthesis ($r = 0.793$; $n = 40$; $p < 0.001$; Spearman's correlation; two-tailed t test; see Figure 2). The mean respiratory quotient (RQ, defined as the molar $\Delta CO_2/\Delta O_2$) and photosynthetic quotient (PQ; defined as the molar $\Delta O_2/\Delta CO_2$) were 0.85 ± 0.24 (1σ) and 1.24 ± 0.53 (1σ), respectively. The mean RQ and PQ were similar to those established earlier in the season on the same glaciers of 0.80 ± 0.17 (1σ) and 1.24 ± 0.20 (1σ), respectively [*Telling et al.*, 2010].

[17] Rates of gross photosynthesis and respiration in water only incubations were close to the detection limit and lower than those of bottles with cryoconite added (Figure 3). Rates of gross photosynthesis and respiration in incubations amended with cryoconite were 588.9 ± 327.4 (1σ) $\mu g\ C\ l^{-1}\ d^{-1}$ (18.7 ± 10.3 $\mu g\ C\ g^{-1}\ d^{-1}$) and 655.7 ± 392.0 $\mu g\ C\ l^{-1}\ d^{-1}$ (1σ) (18.7 ± 9.1 $\mu g\ C\ g^{-1}\ d^{-1}$), respectively (Figure 4). Rates of NEP in bottles amended with cryoconite ranged from net autotrophy (maximum of 170.5 $\mu g\ C\ L^{-1}\ d^{-1}$, or 10.6 $\mu g\ C\ g^{-1}\ d^{-1}$) to net heterotrophy (minimum of -997.9 $\mu g\ C\ L^{-1}\ d^{-1}$, or -11.7 $\mu g\ C\ g^{-1}\ d^{-1}$). The mean rate of NEP in all bottles amended with cryoconite was close to balance at -45.7 ± 216 0.2 $\mu g\ C\ L^{-1}\ d^{-1}$ (1σ) (-0.12 ± 4.1 $\mu g\ C\ g^{-1}\ d^{-1}$; see Figure 4).

3.2. Cryoconite Hole Physical Dimensions and Organic Chemistry

[18] The mean cryoconite water volume: cryoconite sediment volume of cryoconite holes on AB, ML and VB ranged between ~31:1 and 42:1 (Table 1), within a factor of two of the typical ~60:1 ratio used in the bottle incubations. The mean thickness of cryoconite used in the in situ incubations was 2.9 ± 1.8 mm (1σ), with a range from 1 mm up to 8 mm (Figure 4d). The TOC of cryoconite ranged from 5.0 to 44.5 mg C g^{-1} sediment (0.5 to 4.5% by sediment weight; see Figure 4e). Mean TOC values for AB, ML, and VB cryoconite were 17.3, 20.1, and 33.9 mg C g^{-1}, respectively. The three moraine samples from ML had TOC concentrations of 7.7 ± 10.0 mg C g^{-1}(1σ), 4.2 ± 0.8 mg C g^{-1} (1σ) and 2.9 ± 10.2 mg C g^{-1}(1σ), with a mean value for all three samples of 4.9 ± 2.8 mg C g^{-1} (1σ). The chlorophyll *a* content of cryoconite ranged from 2.1 to 23.0 $\mu g\ C\ g^{-1}$ (Figure 4f), while no chlorophyll *a* was detected in any of the moraine samples. Chlorophyll *a* and TOC of cryoconite samples were significantly positively correlated ($r = 0.602$; $p < 0.001$; $n = 40$; Spearman's correlation; two-tailed t test).

3.3. Multivariate Analysis

[19] The length of the gradient along the first ordination axis of the data determined by DCCA was 0.54 SD. Since

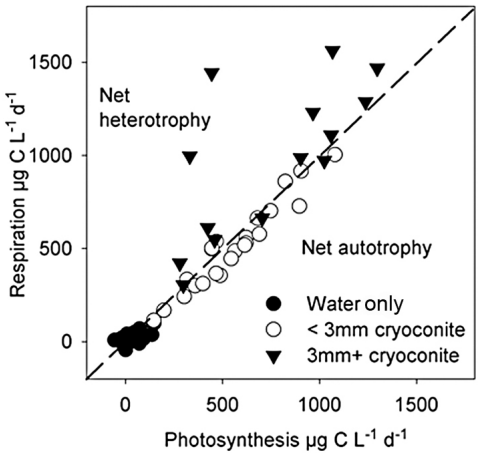

Figure 3. Respiration versus photosynthesis for all data. Water only, cryoconite <3 mm thick, and cryoconite 3+ mm thick are plotted separately. There is a good correlation between photosynthesis and respiration if all cryoconite-amended data are considered ($r = 0.814$; $p < 0.001$; $n = 40$; Spearman's correlation; two-tailed t test) and a stronger correlation if only shallow (<3 mm) are considered ($r = 0.948$; $p < 0.001$; $n = 25$; Spearman's correlation; two-tailed t test).

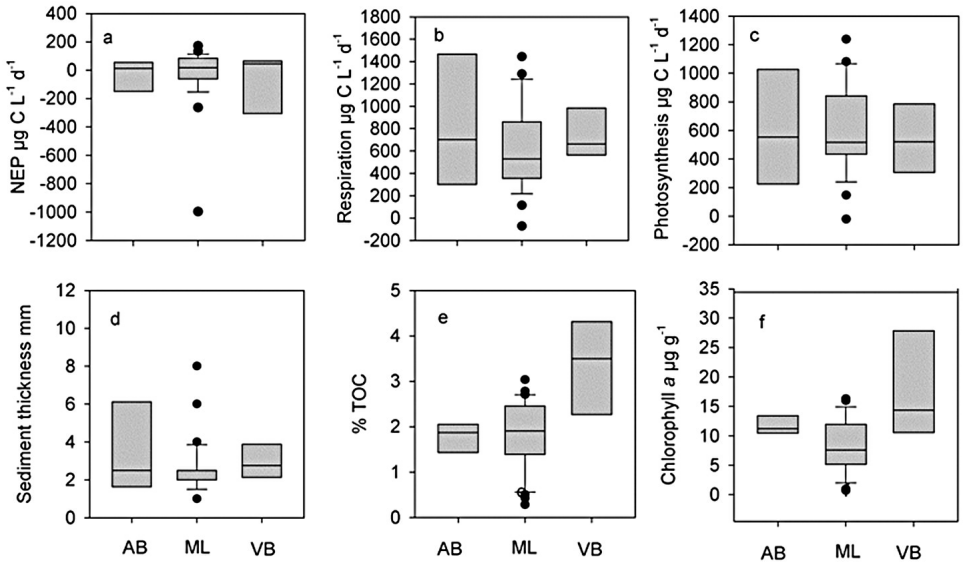

Figure 4. Box plots of data used in multivariate analysis: (a) net ecological production (NEP), (b) respiration, (c) photosynthesis, (d) sediment thickness, (e) total organic carbon (TOC), and (f) chlorophyll *a*. Horizontal line shows the median; bottoms and tops of shaded boxes show the 25th and 75th percentiles, respectively; error bars show the 90th percentiles; and solid dots show individual outliers. AB, Austre Brøggerbreen; ML, Midtre Lovénbreen; VB, Vestre Brøggerbreen.

linear ordination methods are recommended when the gradient length is <3 SD and absolute values are analyzed [*ter Braak and Šmilauer*, 2002; *Ramette and Tiedje*, 2007], the linear constrained ordination method RDA was employed to explain the variation in the microbial activity data.

[20] Figure 5 shows the results of RDA using glaciers and the sediment thickness, TOC and chlorophyll *a* data as independent (explanatory) variables and the photosynthesis, respiration and NEP data (in units of volume) as dependent (explained) variables. The analysis explained a total of 58.7% of the data variation and identified three significant ($p < 0.05$) controls on microbial production: sediment thickness accounted for 36.3% ($p = 0.002$; $F = 17.65$), TOC concentration for 14.6% ($p = 0.004$; $F = 8.88$) and VB for 5.6% ($p = 0.046$; $F = 3.70$).

[21] Table 2 shows the results of three RDAs that used photosynthesis, respiration and NEP on a volume basis, as the only dependent variable and all the environmental variables as independent variables. While TOC was the only variable significantly explaining the variation in the photosynthesis data, respiration was significantly affected by the concentration of TOC and sediment thickness and also the locality of VB explained a significant portion of the variation. The only significant control of NEP in our analysis was sediment thickness, accounting for more than half of the variation within the data (Table 2).

3.4. Cryoconite Thickness Experiments

[22] In each of the five cryoconite thickness experiments NEP was net autotrophic (rates of photosynthesis greater than respiration) at cryoconite thicknesses <3 mm, with trends toward net heterotrophy with increasing cryoconite thickness (Figure 6). Slopes of best fit linear regression lines for NEP were significantly less than zero in all cases ($p < 0.05$; two-tailed t test). This further corroborates the inverse relationship between cryoconite thickness and NEP documented for in situ cryoconite holes (Figure 5). The mean cryoconite thickness where NEP = 0 for all five experiments was 3.0 mm ± 1.2 mm (1σ).

4. Discussion

4.1. Controls on Rates of Respiration and Photosynthesis on Svalbard Valley Glaciers

[23] There were significant ($p < 0.05$) correlations between rates of respiration (in units of volume) with both sediment thickness and organic carbon, explaining a combined total of 72.7% of total variation in the respiration rates (Table 2). The significant increase in respiration with increasing sediment depth is likely due to increases in both the amount of labile organic matter and number of microbial cells within the incubations, since cryoconite samples were added to the bottles in bulk. The simplest explanation for the significant correlation between TOC and respiration is that a relatively constant fraction of TOC between sites is bioavailable, and hence increasing TOC increases the amount of available carbon for respiration. The reason for the small (6.8% of total variation; see Table 1) but significant negative relationship of VB site to respiration (Figure 5) is unclear. One possibility is that cryoconite holes on VB contain a higher

Table 1. Physical Dimensions of Studied Cryoconite Holes[a]

Glacier	Cryoconite Hole Area (cm^2)	Cryoconite Hole Water Depth (cm)	Cryoconite Thickness (mm)	Volume Water: Volume Cryoconite
AB ($n = 8$)	48.4 ± 19.4	8.3 ± 2.3	3.0 ± 2.0	40.6 ± 22.9
ML ($n = 24$)	51.1 ± 34.7	5.8 ± 3.2	2.7 ± 0.9	31.4 ± 26.6
VB ($n = 8$)	65.0 ± 56.0	6.1 ± 6.0	2.8 ± 3.0	42.0 ± 61.1

[a]Values are means ±1σ.

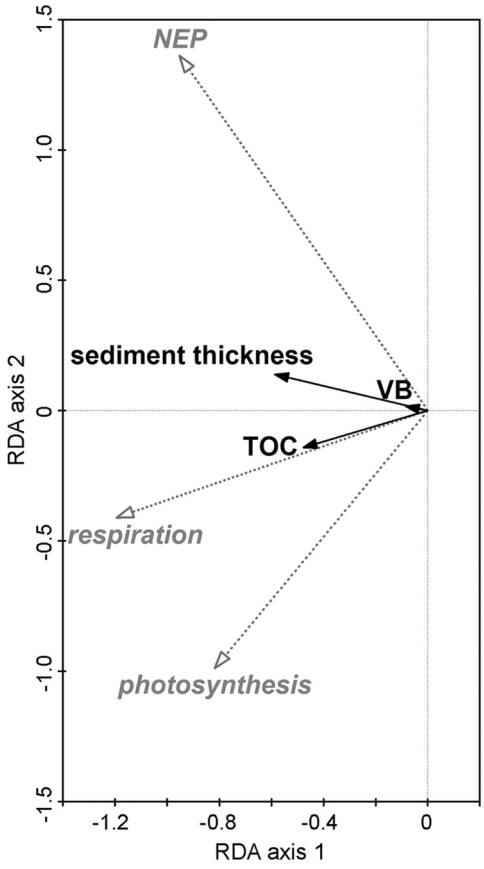

Figure 5. Results of RDA using glaciers and the sediment thickness, total organic carbon (TOC), and chlorophyll *a* data as independent (explanatory) variables (solid lines) and the photosynthesis, respiration, and NEP data as dependent (explained) variables (dotted lines). VB, Vestre Brøggerbreen. Chlorophyll *a* and the glaciers Midtre Lovénbreen and Austre Brøggerbreen were not significant ($p < 0.05$) explanatory variables. Note that during the data transformation prior to RDA, the sign of NEP was changed; hence the positive correlation between sediment thickness and NEP is actually negative.

proportion of refractory to labile carbon, although we have no data to further test this hypothesis.

[24] The lack of any significant relationship ($p < 0.05$) between photosynthesis (in units of volume) and sediment thickness is consistent with light limitation within deeper sediment layers. Incident PAR is typically completely attenuated at thicknesses of <1 mm in silty sediments restricting photosynthesis to the upper submillimeter depth of sediment grains [*Jorgensen and DesMarais*, 1986; *Garcia-Pichel and Bebout*, 1996]. The significant correlation ($p < 0.05$) of TOC with photosynthesis, accounting for 26.1% of the total variation of photosynthesis (Table 2), is unlikely to be because in situ photosynthesis within the cryoconite holes forms the majority of TOC. We show in section 4.3 that the measured rates of NEP are unlikely to be able to produce more than a small fraction of TOC within the studied cryoconite holes on a reasonable timeframe. An alternative explanation for the positive correlation between TOC and photosynthesis is that the breakdown of organic matter allochthonous to the cryoconite holes (although potentially produced autochthonously elsewhere on the glacier) is supporting photoautotrophic growth, perhaps by the supply of essential nutrients such as nitrogen or phosphorus [*Tranter et al.*, 2004; *Stibal et al.*, 2008b, 2009].

[25] Less than half of the variation in rates of gross photosynthesis could be explained by the measured variables in this study (Table 2), indicating that additional factors are likely important. One key missing variable measured in this study for explaining rates of gross photosynthesis is the availability of photosynthetically active radiation (PAR), which changes with season, cloud cover, and shading effects by cryoconite hole walls and local topography [*Hodson et al.*, 2010b]. The availability of nutrients such as phosphorus and nitrogen may also be an important factor for microbial growth and activity [*Stibal et al.*, 2008b; *Telling et al.*, 2011]. Phosphorus has previously been shown to be limiting in the water phase of cryoconites [*Mindl et al.*, 2007]. Further, some cryoconite holes on AB, ML and VB can become depleted in available aqueous and sediment-bound nitrogen resulting in microbial nitrogen fixation [*Telling et al.*, 2011]. Microbial nitrogen fixation could feasibly have a negative impact on rates of microbial growth and activity since it is an energetically costly process relative to the uptake of aqueous nitrogen species [*Gutschick*, 1978; *Telling et al.*, 2011].

[26] The strong positive correlation between respiration and photosynthesis in cryoconite holes, with a tendency to net autotrophy within <3 mm thick sediments (Figure 3), is consistent with a closely coupled microbial carbon loop where labile carbon produced by phototrophs supports the majority of the measured rates of respiration [*Hodson et al.*, 2010a]. Therefore while the majority of organic carbon within Svalbard cryoconite holes is not likely formed in situ within the holes via photosynthesis (see section 4.3), conversely the recycling of labile organic carbon produced by photosynthesis within cryoconite holes may support a significant fraction of the total microbial activity within the holes.

4.2. Controls on Net Ecosystem Production on Svalbard Valley Glaciers

[27] The only significant ($p < 0.05$) measured environmental control on NEP was sediment thickness, accounting for 55.7% of total NEP variation (Table 2). The strong

Table 2. Results of RDAs With Manual Forward Selection Using Photosynthesis, Respiration, and NEP as the Only Dependent Variable[a]

	Variation Explained (%)	*p* Value	*F* Value
Photosynthesis	40.2		
1 TOC	26.1	0.002	10.95
Respiration	72.7		
1 TOC	41.8	0.002	22.22
2 sediment thickness	24.1	0.002	21.16
3 Västre Brøggerbreen	6.8	0.010	7.16
Net ecosystem production	63.2		
1 sediment thickness	55.7	0.002	39.02

[a]Independent variables were included in analysis according to their percentage of variation explained. Only significant controls ($p < 0.05$) are shown.

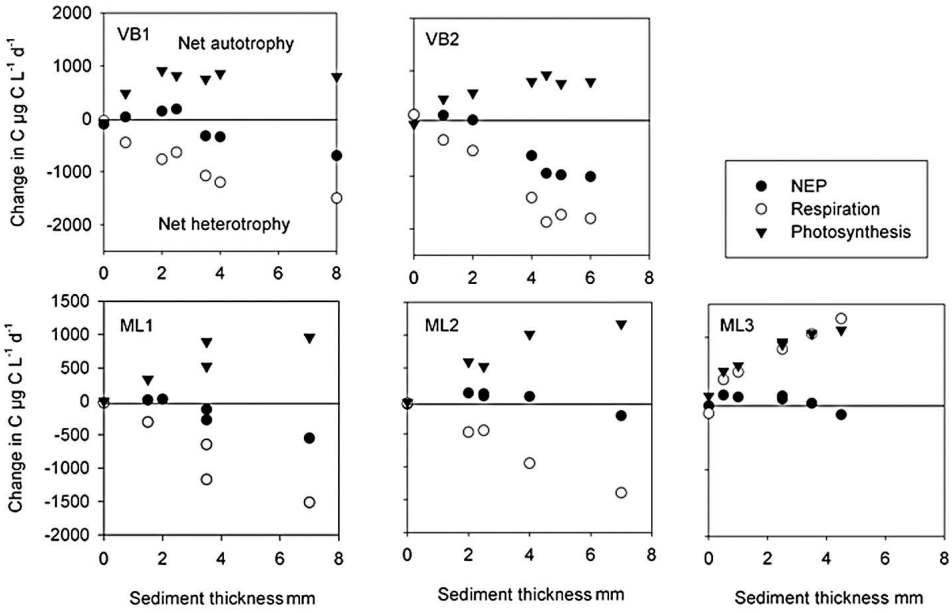

Figure 6. Results of cryoconite thickness experiments carried out on Midtre Lovénbreen (ML1, ML2, and ML3) and Vestre Brøggerbreen (VB1 and VB2). Graphs show the change in rates of gross photosynthesis, respiration, and net ecosystem production (NEP) as a function of cryoconite thickness. The smallest grain sizes (0.5 to 1 mm) represent the thickness of a single cryoconite grain.

control of sediment thickness on NEP is clearly shown in Figures 3 and 6 and indicates that NEP in cryoconite holes tends to net autotrophy at sediment thicknesses of <3 mm (where rates of photosynthesis are typically greater than rates of respiration) and toward net heterotrophy at sediment thicknesses of >3 mm (where rates of respiration typically exceed those of photosynthesis). The relative increase in respiration over photosynthesis at sediment depths >3 mm (Figures 3 and 6) may be explained by light limitation in thicker sediments owing to shading by cryoconite grains.

[28] The mean rate of NEP on the valley glaciers (-0.12 ± 4.1 μg C g^{-1} d^{-1}) was slightly net heterotrophic, although close to the detection limit. Although there appears to be little or no overall accumulation of autochthonous organic carbon in the cryoconite holes of this study, there are likely to be loci of net autotrophy and net heterotrophy which are strongly controlled by sediment thickness. Importantly, cryoconite debris in hydrologically isolated cryoconite holes on Arctic glaciers tend to form uniform one grain layers owing to the effect of lateral as well as vertical melting of ice by cryoconite grains heated by solar radiation [*Cook et al.*, 2010]. There may therefore be a tendency for net autotrophy in more hydrologically stable regions with lower slopes and less water flow, allowing time for cryoconite to equilibrate to a one grain thick layer. Conversely, cryoconite holes with higher slopes and more rapid streamflow may have a tendency toward net heterotrophy owing to greater flushing of cryoconite holes and the subsequent piling up of thicker sediment. For example, a previous glacier wide survey of cryoconite coverage on ML toward the end of the main melt season demonstrated that cryoconite holes on the lower half of ML (where cryoconites in this study were focused; see Figure 1) were dominated by stream cryoconite holes with relatively high rates of supraglacial flushing, while the upper half of ML was dominated by relatively isolated cryoconite holes with relatively low rates of supraglacial flow [*Hodson et al.*, 2007]. The potential for organic carbon from autochthonous origin to accumulate at higher and less hydrologically disturbed parts of the Greenland Ice Sheet ablation zone has been recently demonstrated [*Stibal et al.*, 2012]. We hypothesize that rates of significant net organic production on ML may therefore be focused in the upper half of ML where thin one grain layer cryoconite may dominate. Furthermore different surface regions on valley glaciers may switch between overall net autotrophy to net heterotrophy throughout the melt season owing to changes in the hydrological regime.

4.3. Sources of Organic Matter in Svalbard Cryoconite Holes

[29] We assess the potential importance of net autotrophy for producing organic carbon in thin (1 to <3 mm thick) cryoconite layers using equation (1):

$$Melt\,seasons = \frac{(\text{Cryconite organic carbon}) - (\text{moraine organic carbon})}{(\text{NEP} \times \text{time})} \quad (1)$$

where melt seasons is the number of melt seasons to produce the TOC or estimated phototroph biomass of the cryoconite hole, cryoconite organic carbon (in units of μg C g^{-1}) is either TOC or estimated phototroph biomass (the latter estimated by converting the measured concentrations of chlorophyll *a* to phototroph carbon biomass using a ratio of 1:47) [*Riemann et al.*, 1989], moraine organic carbon is the mean TOC value of moraine debris on ML (4900 μg C g^{-1}), NEP is in units of μg C g^{-1} d^{-1} for holes with autotrophic growth only, and time is the typical length of a melt season on ML (60 days) [*Hodson et al.*, 2007]. Although the moraine

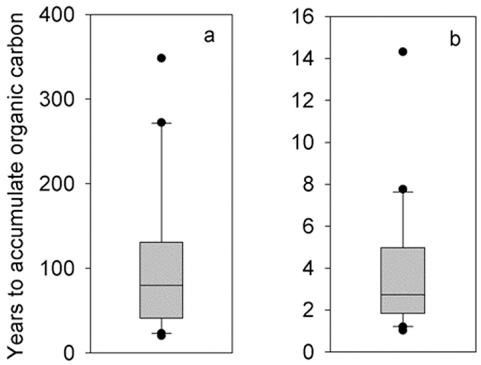

Figure 7. Estimates of the number of melt seasons required to produce organic carbon in thin (<3 mm thick) autotrophic cryoconite sediment: (a) time required to form total organic carbon and (b) time required to form the estimated phototroph carbon biomass of cryoconite. These time estimates were calculated using equation (1) (see section 4.3). Phototroph biomass was estimated by assuming a 1:47 ratio between the measured chlorophyll *a* concentrations of cryoconite and phototroph carbon biomass (after *Riemann et al.* [1989]; see section 4.3).

organic carbon values in equation (1) are based on just three samples of a lateral moraine from ML, their low TOC values (relative to cryoconite) are consistent with previous reports of moraine from the glaciers. A value of 3000 μg C g^{-1} has been reported from lateral moraine on ML [*Borin et al.*, 2010], while the TOC content of barren soils and subglacial derived sediment in the forefields of VB, ML and AB has been reported as typically below detection (<1% dry weight) while cryoconite debris TOC on the three glaciers was typically several percent dry weight [*Kaštovská et al.*, 2005].

[30] The mean time needed to form the estimated phototroph biomass in thin (1 to <3 mm sediment thickness) autotrophic cryoconite holes is 3.3 $\pm$ 3 years (1σ), with a minimum of 1 year and maximum of 14 years (Figure 7). The mean time required to form the mean TOC in the same holes is 105 $\pm$ 91 years (1σ), with a minimum of 20 years and a maximum of 348 years (Figure 7). The typical residence time of cryoconite in stream washed holes on Svalbard valley glaciers has been estimated to on the order of <1 year to several years [*Stibal et al.*, 2008a; *Hodson et al.*, 2010a]. Thin (1 to <3 mm) cryoconite sediments on Svalbard valley glaciers may therefore have sufficiently high rates of autochthonous carbon production to support the growth of a relatively small (compared to TOC) phototrophic biomass, but likely not more than a fraction of their TOC. More hydrologically stable (isolated) cryoconite holes elsewhere however could have substantially greater residence times on the ice surface, and hence a greater potential for autochthonous organic matter accumulation. For example, cryoconite on sections of the Greenland Ice Sheet may have a residence time of >100 years on the ice surface [*Nobles*, 1960], and autochthonous organic carbon production provides one explanation for the higher TOC content of cryoconite debris documented on parts of the Greenland Ice Sheet (e.g., 13–20% TOC by dry weight) [*Gerdel and Drouet*, 1960] relative to Svalbard valley glaciers (Figure 4).

[31] The above calculations indicate that at the time of sampling overall rates of net autochthonous organic carbon production within the cryoconite holes were unable to account for the majority of organic matter in the cryoconite. This discrepancy in the organic carbon budget of the cryoconite holes can be explained in one of three ways. First, there may be allochthonous inputs of organic carbon from environments external to the glacier into the cryoconite holes. Second, there may be autochthonous organic carbon production in alternative supraglacial habitats on the glacier surface which is subsequently washed into the cryoconite holes. Third, NEP rates in nascent cryoconite holes may have been substantially higher than in the holes at the time of sampling.

[32] Input of allochthonous organic carbon into cryoconite holes is likely, although the magnitude of this flux is currently unknown. Windblown organic matter from adjacent tundra [*Stibal et al.*, 2008a] is perhaps the most likely source. There may also be input of organic carbon near the terminus of the glaciers however from subglacial debris pushed up to the surface in the form of pressure ridges, although reported values of for subglacial debris samples at the front of AB, ML and VB are low (<1% TOC dry weight) [*Kaštovská et al.*, 2005].

[33] The autochthonous production of organic carbon in alternative habitats on the glacier surface, and subsequent washing into cryoconite holes, is also feasible. The snowpack overlies the entire surface of Svalbard valley glaciers at the start of the season and retreats upslope as the melt season progresses [*Hodson et al.*, 2008], while dispersed cryoconite lying on the ice surface can constitute up to half of the total mass of cryoconite on Svalbard valley glaciers [*Hodson et al.*, 2007]. The NEP of the snowpack and dispersed cryoconite environments is currently unknown [*Hodson et al.*, 2008] but could potentially be significant [*Takeuchi*, 2002; *Hodson et al.*, 2007].

[34] The third explanation for the source of organic carbon in cryoconite holes is that rates of NEP are greater in nascent cryoconite holes than in more mature cryoconite holes. This mechanism appears plausible but is currently untested. Microimaging of cryoconite grains indicates that cryoconite in cryoconite holes is typically composed of individual small grains of $\leq$ 100 μm or less bound together in larger aggregates by exopolysaccharides [*Takeuchi et al.*, 2001; *Hodson et al.*, 2010a; *Langford et al.*, 2010]. Given the negative relationship between cryoconite thickness and NEP (Figures 5 and 6), it is plausible that rates of photosynthesis could dominate over respiration in the initial phase of aggregation resulting in relatively high rates of NEP. In contrast the more mature cryoconite grains in the cryoconite holes of this study had a relatively close balance between photosynthesis and respiration (Figure 3). The lack of cryoconite <0.5 mm thick in the cryoconite holes of this study (Figures 4d and 6) tends to suggest however that either the initial aggregation of cryoconite debris is extremely rapid, or that the initial aggregation does not occur within the cryoconite holes themselves but instead within either the snowpack and/or dispersed cryoconite debris on the ice surface [*Langford et al.*, 2010]. Some support for the latter comes from a previous study on an Antarctic glacier that demonstrated a threshold aggregation size is necessary before cryoconite can absorb sufficient solar energy to melt into the ice to form cryoconite holes

[*MacDonell and Fitzsimons*, 2008]. It is possible that a similar threshold aggregation size mechanism operates on Arctic valley glaciers.

5. Conclusions

[35] Cryoconite thickness and organic matter were significant controls on rates of respiration (in units of volume) in cryoconite holes on three Svalbard valley glaciers. Organic matter (but not sediment depth) was a significant control on photosynthesis. Sediment depth explained over half the variation of net ecosystem production (NEP), with net autotrophic rates typical only in sediment <3 mm thick. The measured rates of NEP were not sufficient to account for the organic matter which has likely accumulated in the cryoconite holes on timescales of less than decades, suggesting that either (1) the glacier surface receives allochthonous organic material from surrounding environments, or (2) organic matter is derived from in-washed autochthonous material from alternative habitats (e.g., the snowpack and dispersed cryoconite) on the glacier surface, or (3) organic carbon accumulated in the hole during a nascent period, when rates of NEP were much higher. The cycling of autochthonous labile carbon produced by phototrophs within cryoconite holes may sustain a significant proportion of the total in situ microbial activity within cryoconite holes.

[36] **Acknowledgments.** This work was funded by grants awarded to A.M.A. and A.H. from NERC (NE/G00496X/1 and NE/G006253/1). We are grateful to three anonymous reviewers and the Associate Editor, whose comments greatly strengthened this paper. We would like to thank Nick Cox for his logistical help at NERC Arctic station Ny-Ålesund.

References

Anesio, A. M., A. J. Hodson, A. Fritz, R. Psenner, and B. Sattler (2009), High microbial activity on glaciers: Importance to the global carbon cycle, *Global Change Biol.*, *15*, 955–960, doi:10.1111/j.1365-2486.2008.01758.x.

Bøggild, C. E., R. E. Brandet, K. J. Brown, and S. G. Warren (2010), The ablation zone in north east Greenland: Ice types, albedos and impurities, *J. Glaciol.*, *56*, 101–113, doi:10.3189/002214310791190776.

Borin, S., et al. (2010), Rock weathering creates oases of life in a high Arctic desert, *Environ. Microbiol.*, *12*, 293–303, doi:10.1111/j.1462-2920.2009.02059.x.

Christner, B. C., B. H. Kvitko, and J. N. Reeve (2003), Molecular identification of Bacteria and Eukarya inhabiting an Antarctic cryoconite hole, *Extremophiles*, *7*, 177–183, doi:10.1007/s00792-002-0309-0.

Cook, J., A. Hodson, J. Telling, A. Anesio, T. Irvine-Fynn, and C. Bellas (2010), The mass–area relationship within cryoconite holes and its implications for primary production., *Ann. Glaciol.*, *51*, 106–110. [Available at http://www.igsoc.org/annals/v51/56/a56a009.pdf.]

Edwards, A., A. M. Anesio, S. M. Rassner, B. Sattler, B. P. Hubbard, W. T. Perkins, M. Young, and G. W. Griffith (2011), Possible interactions between bacterial diversity, microbial activity and supraglacial hydrology of cryoconite holes in Svalbard, *ISME J.*, *5*, 150–160, doi:10.1038/ismej.2010.100.

Garcia-Pichel, F., and B. M. Bebout (1996), Penetration of ultraviolet radiation into shallow water sediments: High exposure for photosynthetic communities, *Mar. Ecol. Prog. Ser.*, *131*, 257–262, doi:10.3354/meps131257.

Gerdel, R. W., and F. Drouet (1960), The cryoconite of the Thule area, Greenland, *Trans. Am. Microsc. Soc.*, *79*, 256–272.

Gutschick, V. P. (1978), Energy and nitrogen fixation, *BioScience*, *28*, 571–575, doi:10.2307/1307512.

Hagen, J. O., J. Kohler, K. Melvold, and J. G. Winther (2003), Glaciers in Svalbard: Mass balance, runoff and freshwater flux, *Polar Res.*, *22*, 145–159, doi:10.1111/j.1751-8369.2003.tb00104.x.

Hodson, A., et al. (2007), A glacier respires: Quantifying the distribution and respiration CO_2 flux of cryoconite across an entire Arctic supraglacial ecosystem, *J. Geophys. Res.*, *112*, G04S36, doi:10.1029/2007JG000452.

Hodson, A., A. M. Anesio, M. Tranter, A. Fountain, M. Osborn, J. Priscu, J. Laybourn-Parry, and B. Sattler (2008), Glacial ecosystems, *Ecol. Monogr.*, *78*, 41–67, doi:10.1890/07-0187.1.

Hodson, A., K. Cameron, C. Bøggild, T. Irvine-Fynn, H. Langford, D. Pearce, and S. Banwart (2010a), The structure, biological activity and biogeochemistry of cryoconite aggregates upon an Arctic valley glacier: Longyearbreen, Svalbard, *J. Glaciol.*, *56*, 349–362, doi:10.3189/002214310791968403.

Hodson, A., C. Bøggild, E. Hanna, P. Huybrechts, H. Langford, K. Cameron, and A. Houldsworth (2010b), The cryoconite ecosystem on the Greenland ice sheet, *Ann. Glaciol.*, *51*, 123–129, doi:10.3189/172756411795931985.

Hood, E., J. Fellman, R. G. M. Spencer, P. J. Hernes, R. Edwards, D. D'Amore, and D. Scott (2009), Glaciers as a source of ancient and labile organic matter to the marine environment, *Nature*, *462*, 1044–1047, doi:10.1038/nature08580.

Jorgensen, B. B., and D. J. DesMarais (1986), A simple fiberoptic microprobe for high-resolution light measurements—Application in marine sediments, *Limnol. Oceanogr.*, *31*, 1376–1383, doi:10.4319/lo.1986.31.6.1376.

Kaštovská, K., J. Elester, M. Stibal, and H. Šantrůčková (2005), Microbial assemblages in soil microbial succession after glacial retreat in Svalbard (high Arctic), *Microbial Ecol.*, *50*, 396–407, doi:10.1007/s00248-005-0246-4.

Langford, H., A. Hodson, S. Banwart, and C. Bøggild (2010), The microstructure and biogeochemistry of Arctic cryoconite granules, *Ann. Glaciol.*, *51*, 87–94, doi:10.3189/172756411795932083.

Legendre, P., and L. Legendre (1998), *Numerical Ecology*, 853 pp., Elsevier, Amsterdam.

MacDonell, S., and S. Fitzsimons (2008), The formation and hydrological significance of cryoconite holes, *Prog. Phys. Geogr.*, *32*, 595–610, doi:10.1177/0309133308101382.

Mindl, B., A. M. Anesio, K. Meirer, A. J. Hodson, J. Laybourn-Parry, R. Sommaruga, and B. Sattler (2007), Factors influencing bacterial dynamics along a transect from supraglacial runoff to proglacial lakes of a high Arctic glacier, *FEMS Microbiol. Ecol.*, *59*, 307–317, doi:10.1111/j.1574-6941.2006.00262.x.

Nobles, L. H. (1960), Glaciological investigations, Nunatarssuaq Ice Ramp, northwestern Greenland, Tech. Rep. 66, U.S. Army Corps. of Eng. Cold Reg. Res. Lab., Hanover, N. H.

Nuth, C., J. Kohler, H. F. Aas, O. Brandt, and J. O. Hagen (2007), Glacier geometry and elevation changes on Svalbard (1936–90), a baseline dataset, *Ann. Glaciol.*, *46*, 106–116, doi:10.3189/172756407782871440.

Quesada, A., W. F. Vincent, and D. R. S. Lean (1999), Community and pigment structure of Arctic cyanobacterial assemblages: The occurrence and distribution of UV-absorbing compounds, *FEMS Microbiol. Ecol.*, *28*, 315–323, doi:10.1111/j.1574-6941.1999.tb00586.x.

Ramette, A., and J. M. Tiedje (2007), Multiscale responses of microbial life to spatial distance and environmental heterogeneity in a patchy ecosystem, *Proc. Natl. Acad. Sci. U. S. A.*, *104*, 2761–2766, doi:10.1073/pnas.0610671104.

Riemann, B., P. Simonsen, and L. Stensgaard (1989), The carbon and chlorophyll content of phytoplankton from various nutrient regimes, *J. Plankton Res.*, *11*, 1037–1045, doi:10.1093/plankt/11.5.1037.

Säwström, C., P. Mumford, W. Marshall, A. Hodson, and J. Laybourn-Parry (2002), The microbial communities and primary productivity of cryoconite holes in an Arctic glacier (Svalbard 79°N), *Polar Biol.*, *25*, 591–596, doi:10.1007/s00300-002-0388-5.

Stibal, M., M. Šabacká, and K. Kaštovská (2006), Microbial communities on glacier surfaces in Svalbard: Impact of physical and chemical properties on abundance and structure of cyanobacteria and algae, *Microbial Ecol.*, *52*, 644–654, doi:10.1007/s00248-006-9083-3.

Stibal, M., M. Tranter, L. G. Benning, and J. Rehak (2008a), Microbial primary production on an Arctic glacier is insignificant in comparison with allochthonous organic carbon input, *Environ. Microbiol.*, *10*, 2172–2178, doi:10.1111/j.1462-2920.2008a.01620.x.

Stibal, M., M. Tranter, J. Telling, and L. G. Benning (2008b), Speciation, phase association and potential bioavailability of phosphorus on a Svalbard glacier, *Biogeochemistry*, *90*, 1–13, doi:10.1007/s10533-008-9226-3.

Stibal, M., A. M. Anesio, C. J. D. Blues, and M. Tranter (2009), Phosphatase activity and organic phosphorus turnover on a high Arctic glacier, *Biogeosciences*, *6*, 913–922, doi:10.5194/bg-6-913-2009.

Stibal, M., J. Telling, J. Cook, K. M. Mak, A. Hodson, and A. M. Anesio (2012), Environmental controls on microbial abundance and activity on the Greenland Ice Sheet: A multivariate analysis approach, *Microbial Ecol.*, *63*(1), 74–84, doi:10.1007/s00248-011-9935-3.

Takeuchi, N. (2002), Surface albedo and characteristics of cryoconite (biogenic surface dust) on an Alaska glacier, Gulkana Glacier in the Alaska Range, *Bull. Glaciol. Res.*, *19*, 63–70.

Takeuchi, N., S. Kohshima, and K. Seko (2001), Structure, formation, and darkening process of albedo-reducing material (cryoconite) on a Himalayan glacier: A granular algal mat growing on the glacier, *Arct. Antarct. Alp. Res.*, *33*, 115–122.

Takeuchi, N., Y. Matsuda, A. Sakai, and A. Fujita (2005), A large amount of biogenic surface dust (cryoconite) on a glacier in the Qilian Mountains, China, *Bull. Glaciol. Res.*, *22*, 1–8.

Telling, J., A. M. Anesio, J. Hawkings, M. Tranter, J. L. Wadham, A. J. Hodson, T. Irvine-Fynn, and M. L. Yallop (2010), Measuring rates of gross photosynthesis and net community production in cryoconite holes: A comparison of field methods, *Ann. Glaciol.*, *51*, 153–162, doi:10.3189/172756411795932056.

Telling, J., A. M. Anesio, M. Tranter, T. Irvine-Fynn, A. Hodson, C. Butler, and J. Wadham (2011), Nitrogen fixation on Arctic glaciers, Svalbard, *J. Geophys. Res.*, *116*, G03039, doi:10.1029/2010JG001632.

ter Braak, C. J. F., and P. Šmilauer (2002), *CANOCO Reference Manual and CanoDraw for Windows User's Guide: Software for Canonical Community Ordination (Version 4.5)*, 550 pp., Microcomput. Power, Ithaca, N. Y.

Thompson, R. C., M. L. Tobin, S. J. Hawkins, and T. A. Norton (1999), Problems in extraction and spectrophotometric determination of chlorophyll from epilithic microbial biofilms: Towards a standard method, *J. Mar. Biol. Assoc. U. K.*, *79*, 551–558, doi:10.1017/S0025315498000678.

Tranter, M., A. G. Fountain, C. H. Fritsen, W. B. Lyons, J. C. Priscu, P. J. Statham, and K. A. Welch (2004), Extreme hydrochemical conditions in natural microcosms entombed within Antarctic ice, *Hydrol. Processes*, *18*, 379–387, doi:10.1002/hyp.5217.

A. M. Anesio, C. Butler, J. Hawkings, M. Stibal, J. Telling, M. Tranter, and J. Wadham, Bristol Glaciology Centre, School of Geographical Sciences, University of Bristol, Bristol BS8 1SS, UK. (a.m.anesio@bristol.ac.uk)

A. Hodson, Department of Geography, University of Sheffield, Sheffield S10 2TN, UK.

T. Irvine-Fynn, Centre for Glaciology, Institute of Geography and Earth Science, Aberystwyth University, Aberystwyth SY23 3DB, UK.

M. Yallop, School of Biological Sciences, University of Bristol, Bristol BS8 1UG, UK.